J Ind Microbiol Biotechnol (2006) 33: 445–453
DOI 10.1007/s10295-006-0088-1

ORIGINAL PAPER

Scott Frykman · Hiroko Tsuruta · Jorge Galazzo
Peter Licari

Characterization of product capture resin during microbial cultivations

Received: 12 October 2005 / Accepted: 26 November 2005 / Published online: 11 February 2006

Abstract Various bioactive small molecules produced by microbial cultivation are degraded in the culture broth or may repress the formation of additional product. The inclusion of hydrophobic adsorber resin beads to capture these products in situ and remove them from the culture broth can reduce or prevent this degradation and repression. These product capture beads are often subjected to a dynamic and stressful microenvironment for a long cultivation time, affecting their physical structure and performance. Impact and collision forces can result in the fracturing of these beads into smaller pieces, which are difficult to recover at the end of a cultivation run. Various contaminating compounds may also bind in a non-specific manner to these beads, reducing the binding capacity of the resin for the product of interest (fouling). This study characterizes resin bead binding capacity (to monitor bead fouling), and resin bead volume distributions (to monitor bead fracture) for an XAD-16 adsorber resin used to capture epothilone produced during myxobacterial cultivations. Resin fouling was found to reduce the product binding capacity of the adsorber resin by 25–50%. Additionally, the degree of resin bead fracture was found to be dependent on the cultivation length and the impeller rotation rate. Microbial cultivations and harvesting processes should be designed in such a way to minimize bead fragmentation and fouling during cultivation to maximize the amount of resin and associated product harvested at the end of a run.

Keywords Epothilone · Myxobacteria · Adsorber resin · Cyclodextrin · XAD-16

List of symbols d: resin bead diameter (cm) · d_i: impeller diameter (cm) · ICS: impeller collision severity function (g cm^2/s^3) · n: impeller rotational speed (revolutions/s) · TCS: turbulent bead collision severity function (g cm^2/s^3) · v: velocity of bead sized eddies in the turbulent fluid (cm/s) · v_{tip}: velocity of fluid over the outer edge of the impeller blade (cm/s) · V: volume of bioreactor (cm^3) · α: volume fraction of beads (dimensionless) · ε: turbulent power dissipation per mass of liquid (cm^2/s^3) · ρ_b: density of XAD-16 adsorber resin beads (g/cm^3) · ν: kinematic viscosity of medium (cm^2/s)

S. Frykman (✉) · H. Tsuruta · J. Galazzo · P. Licari
Department of Process Science, Kosan Biosciences Inc.,
3832 Bay Center Place, Hayward, CA, 94545, USA
E-mail: frykman@kosan.com
Tel.: +1-510-7315307
Fax: +1-510-7315101

Introduction

The inclusion of stabilization agents during a microbial cultivation can reduce or prevent product degradation and repression. Adsorber resins are often incorporated into myxobacterial, fungal, and actinomycete cultivations to increase the product titers of bioactive natural products. Examples of natural products in which incorporation of an adsorber resin into the production medium enhances product titers include rubradirin, an antibiotic produced by *Streptomyces achromogenes* v. *rubradiris* [15]; BMS-182123, a metabolite produced by *Penicillium chrysogenum* which acts as an inhibitor of tumor necrosis factor α production [21]; migrastatin and isomigrastatin, potential anticancer agents produced by *Streptomyces platensis* [22]; and the jerangolids and ambruticin, novel antifungal compounds produced by the myxobacterium, *Sorangium cellulosum* [7].

One class of these bioactive compounds of particular interest is the epothilones. Epothilones A and B are secondary metabolites that are naturally produced by another strain of *S. cellulosum* [8]. Epothilone D is reported to exhibit a higher therapeutic index than epothilone B [6] and has been produced as the primary metabolite in *S. cellulosum* and a related myxobacterium, *Myxococcus xanthus* [11, 14]. Epothilone D is a potent inhibitor of microtubule depolymerization, with a mechanism of action similar to that of the anti-cancer drug paclitaxel. Cultivations of *S. cellulosum* strain So

ce90 conducted in the absence of a product-stabilizing agent result in product hydroxylation and/or opening of the lactone ring of the epothilones by monooxygenase and/or esterase enzymes [9]. Adsorber resins and cyclodextrins have been used to minimize epothilone degradation during cultivation. The enzyme-catalyzed degradation of unbound epothilone presumably occurs in addition to a solvent-mediated carbonium ion hydrolysis mechanism proposed by Jumaa et al. [10].

These resin beads are often exposed for a long period of time to a dynamic and stressful environment during cultivation, affecting the various properties of the resin beads. Two properties of importance are the product binding capacity of the resin beads and their resistance to destructive physical forces. Both of these resin properties are studied here in an attempt to understand the nature and degree of how the adsorber resin is degraded during cultivation. Characterization of these resin samples allows the optimal design of cultivation and harvest processes to minimize the amount of product lost during a cultivation utilizing an in situ product capture strategy. These resin beads are relatively non-specific in their binding selectivity for the hydrophobic molecules they encounter in the cultivation broth. Fouling of these beads with medium components or other bacterial metabolites will result in reduced binding capacity and a decreased product capture rate by the resin beads.

Similarly, it is important to understand how the fracturing of the resin beads can result in the loss of product. Shear forces around the agitation impeller and collision of the resin beads with one another or with internal bioreactor structures such as the agitation impeller or baffles may cause the breakage of the beads into smaller pieces. Harvest of these resin beads following a bacterial cultivation usually involves passage of the culture broth through a sieving mesh to retain the beads and product and remove the cells and broth. Appropriate sizing of the capture mesh is dependent on the size of the resin beads, the viscosity of the cultivation broth, and the presence and size of insoluble medium components or cell clumps in the broth. Resin particles smaller than the selected mesh size will pass through the mesh, resulting in the loss of any product associated with these fragments.

Materials and methods

Microbial strains

Sorangium cellulosum strain PF1S-9 produces epothilones C and D, through random insertion of a transposon element into the EpoK epoxidase of So ce90 (DSM6773). PF1S-9 cultures were initiated by reviving a 1 ml frozen cell bank vial in a sterile 250 ml Erlenemeyer flask containing 50 ml of MF1 seed medium [9 g/l soy protein #1116 (Marcor, Carlstadt, NJ, USA); 6 g/l fructose (Tate and Lyle, London, UK); 0.5 g/l $CaCl_2$–$2H_2O$ (EM Science, Gibbstown, NJ, USA); 0.5 g/l $MgSO_4$–$7H_2O$ (EM Science); and 25 mM HEPES buffer (EM Science)] for 4 days at 34°C and 190 rpm. Description of the engineering of *M. xanthus* strain K111-40.1, which also produces epothilones C and D, is as described by Julien and Shah [11].

Batch shake flask production of epothilones

Two grams of XAD-16 resin (Rohm and Haas, Philadelphia, PA, USA) were autoclaved at 121°C for 30 min in a 250 ml unbaffled Erlenmeyer flask with 5 ml of deionized water. The excess water was then removed from the flask, and 50 ml of sterile SF1-P medium [3 g/l soy protein; 6 g/l fructose; 1 g/l $CaCl_2{\cdot}2H_2O$; 1 g/l $MgSO_4{\cdot}7H_2O$; 50 mM HEPES buffer; and 8 ml/l of a 14.6 g/l $FeCl_3$ solution (Sigma, St. Louis, MO, USA)] were added. The control flasks and flasks containing the cyclodextrins contained no XAD-16 resin, only the same amount (50 ml) of SF1-P medium. The 2-hydroxypropyl-α (56330), -β (56332), and -γ (56334) cyclodextrins were obtained from Fluka Chemika (Buchs SG, Switzerland). The production flasks were inoculated with 2.5 ml of the seed culture and incubated at 34°C and 190 rpm for 7 days, followed by flask harvest and processing. One-milliliter samples of culture broth were taken daily and extracted in an equivalent amount of methanol for epothilone titer analysis.

Resin binding capacity studies

Two grams of either fresh or spent (unused or used) resin was placed into a 50 ml conical tube. Exactly 250 mg of epothilone D was weighed out on an analytical balance, suspended in 25 ml of deionized water, and the resulting slurry poured into the conical tube. Additional deionized water was used to wash all of the remaining epothilone D into the conical tube, and sufficient deionized water was added to make the volume in the tube exactly 50 ml. These tubes were placed horizontally in a flask clamp within a 34°C upright shaker, and agitated for 10 days. The resin was washed with deionized water after this loading period and the quantity of epothilone bound to the resin determined as described below.

Culture broth viscosity, oil, and epothilone titer analyses

Culture broth viscosity was determined using an Oswald viscometer (#66044-007; VWR, Brisbane, CA, USA), according to the manufacturer's instructions. All reported measurements were made in triplicate at 34°C, using deionized water as a reference standard. Kinematic broth viscosities were calculated using the following equation:

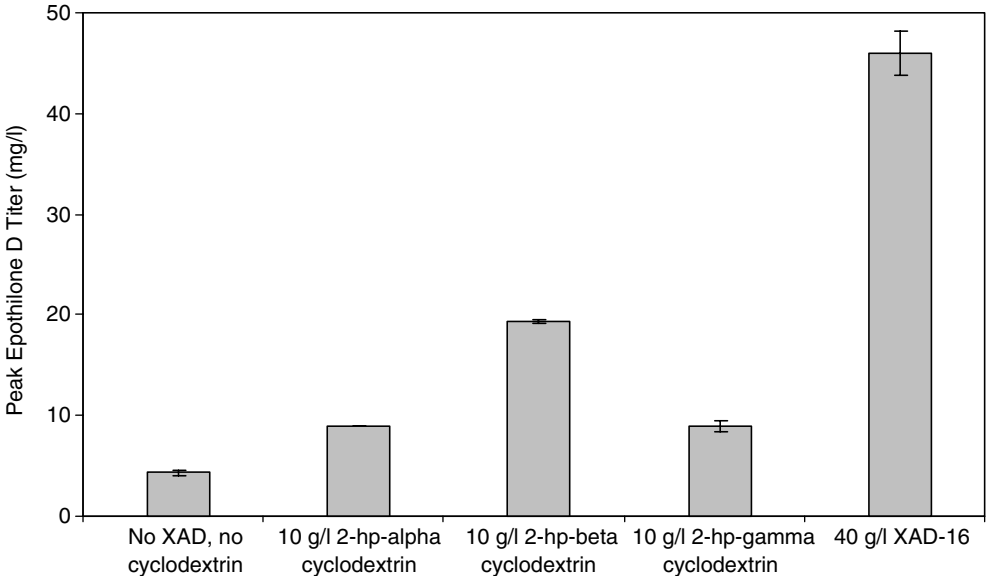

Fig. 1 Inclusion of cyclodextrin or XAD-16 adsorber resin in batch epothilone D production cultures results in enhanced product titers over the control condition (No XAD, no cyclodextrin). *Error bars* indicate the standard deviation of each triplicate data set

$$\text{Broth viscosity} = v\frac{t_1}{t_2}. \quad (1)$$

Here, v = kinematic viscosity of water at 34°C (0.007 cm^2/s); t_1 = averaged measured broth transit time (s); and t_2 = averaged measured water transit time (s).

Epothilone D titers were determined in the following manner. The resin from the flasks or resin binding studies was separated from the cultivation broth by decanting, washed once with deionized water, again followed by decanting of the water. The resin was extracted in 50 ml of reagent-grade methanol for 30 min, and the epothilone C and D titers of the extract quantitated by HPLC. The methanol-extracted culture broth from the cyclodextrin study and the methanol-extracted slurry from the resin binding study were analyzed in the same manner. HPLC analysis was performed using a Hewlett-Packard 1090 HPLC (Palo Alto, CA, USA) with UV detection at 270 nm. A 25 μl aliquot of the methanol-extracted solution was injected across a 4.6×10 mm guard column (MetaChem Inertsil C18 ODS 3, 5 μm, Ansys, Lake Forest, CA, USA), and a longer column of the same material for chromatographic separation (4.6×150 mm). The method was isocratic with 70% acetonitrile and 30% water, and had a total run time of 12 min at a flow rate of 1.0 ml/min.

Quantitation of the amount of methyl oleate bound to a sample of the spent resin was determined in the following manner. A 1 μl sample of the methanol resin extract or a methyl oleate/methanol standard sample was analyzed using an Agilent 6890 GC chromatograph equipped with an Agilent 5973N single-quadrapole mass spectrometer detector and a CTC Analytics Combi PAL autosampler. The chromatographic column was a model HP5-ms (30 m×0.25 mm×0.25 μm, Agilent Technologies, Palo Alto, CA, USA), using helium as the carrier gas with a flow rate of 1 ml/min. The inlet temperature was set at 250°C and the internal temperature gradient for each sample was held at 150°C for 5 min, ramped to 240°C over 10 min, and held at 240°C for 5 min. Methane was used as the reagent gas in the mass spectrometer, and the source and quadrapole temperatures were set at 250 and 150°C, respectively.

Bioreactor resin fracture simulation study

Approximately, 200 g of XAD-16 adsorber resin (density of 1.06 g/ml; median particle diameter of 600 μm) was added to deionized water to a total volume of 5 l in a bioreactor (B-5, B. Braun, Allentown, PA, USA). The dimensions of the working volume of this bioreactor are 15.5 cm in diameter and 27 cm high. The bioreactor was unbaffled, with vessel agitation provided by three-six-bladed Rushton impellers (6.5 cm impeller diameter, and an impeller blade width of 1.8 cm). These impellers were spaced approximately 5 cm apart on the bioreactor drive shaft. Airflow was constant in the bioreactor at 2 l/min, and the temperature maintained at 34°C. The agitation rate profile during the 14 days run was varied to mimic that of an actual myxobacterial epothilone D production cultivation. A 70% glycerol solution was pumped in at an appropriate rate throughout the run to replicate the viscosity profile typically observed during this microbial cultivation. Approximately, 250 ml of the resin/water/glycerol solution was sampled from the bioreactor at various points (days 3, 7, 10, and 14) during the run for resin sizing analysis.

Laser diffraction particulate sizing analysis

Resin size distribution analysis was performed at Malvern Instruments (Southborough, MA, USA) using a Mastersizer 2000. This instrument can detect particles between 0.02 and 2000 μm in diameter. Each reported

distribution is the average of 4–7 measurements of a particular resin/water sample.

Results and discussion

Assessment of epothilone stabilization agents during myxobacterial cultivations

Fermentation products subject to degradation or repression of further production can be stabilized in situ by the addition of a stabilizing agent to sequester the product from degradative enzymes or from the cells. Two such stabilization agents are solid-phase adsorber resins composed of a hydrophobic polymer and the soluble cyclodextrins. When these agents were tested in a batch *S. cellulosum* epothilone production model, each of these compounds enhanced epothilone D product titers over those observed in control cultivations containing no stabilization agents (Fig. 1). Three cyclodextrins of varying molecular weights were tested against each other at a concentration of 10 g/l. Increasing the cyclodextrin concentration beyond this level did not result in higher epothilone titers (data not shown). The 2-hydroxypropyl-beta cyclodextrin resulted in the highest epothilone peak titer of the various cyclodextrins tested, approximately five times higher than the control condition and two times higher than the other two cyclodextrins. This is presumably due to the internal cavity of this cyclodextrin being most appropriately sized for the epothilone D molecule. However, the mean peak titer of the cultivations containing the XAD-16 adsorption resin was 45 mg/l, approximately 2.3 times higher than the mean peak titer observed in the cultivations containing the 2-hydroxypropyl-β cyclodextrin. Product adsorption resin is clearly superior to the cyclodextrins in achieving high titers of epothilone D in this system.

Fouling of product adsorption resin during a microbial cultivation

Despite the resulting high product titers, these XAD-16 resin beads are relatively non-selective in the types of molecules they bind on their surface and have an affinity for any hydrophobic compound. In addition to the desired product, these beads will also bind medium components and other compounds produced by the cells, such as secondary metabolites or pigments. These other compounds occupy binding sites on the beads, thereby "fouling" them and putatively inhibiting the binding of additional epothilone. One example of these fouling compounds is methyl oleate, which is used as a carbon source in *M. xanthus* epothilone production cultivations [14]. GC/MS analysis of resin extracts from an *M. xanthus* cultivation indicate that methyl oleate binds to the resin during a cultivation. During epothilone purification, quantities of this oil elute from the resin, complicating the recovery process [1]. Unlike *M. xanthus, S. cellulosum* has a complete glycolytic pathway and is capable of catabolizing carbohydrates.

Resin samples from the end of fed-batch epothilone production runs of both *M. xanthus* and *S. cellulosum* myxobacteria were tested to determine if the presence of methyl oleate and other putative fouling compounds contributes to or interferes with the binding of additional epothilone to the spent adsorber resins. Resin samples from the end of *S. cellulosum* and *M. xanthus* fed-batch epothilone D production runs were tested to determine the remaining capacity that these resin samples had for further binding of epothilone D. Two grams of resin from representative cultivation runs of each strain was agitated in a 5 g/l epothilone D/water slurry to permit complete saturation of the binding sites on the resin with epothilone. Resin saturation was determined to have occurred when the unbound epothilone concentration in the well-mixed slurry stabilized after approximately 7 days (data not shown).

The initial amount of total epothilone (C and D) bound to each of the spent resins was determined and compared to the total saturation amount of epothilone which could be bound to the fresh resin and the two types of spent resins (Fig. 2). The fresh resin was determined to have an epothilone/resin loading capacity of approximately 80 mg/g. This loading capacity is similar to the 125-mg/g saturation loading at the same resin concentration reported by Yang and Pyle [23] in their study of cephalosporin-C binding to fresh XAD-16 resin. The *M. xanthus* spent resin has a saturation capacity which is approximately 20% lower than the fresh resin (63 mg/g), while the spent resin from the *S. cellulosum* cultivation has a saturation capacity approximately 50% lower than the fresh resin (41 mg/g). There is still excess epothilone binding capacity on both types of spent resins, but the reduction in their binding capacities will result in a decrease in the capture rate of further product. It is also possible that a number of the pores in these spent resin beads have become plugged with cells or other matter, decreasing the pore diffusivity rate of the resin and its contribution to the overall binding rate of the epothilone [23]. This decreased capture rate could then result in an increase in the unbound concentration of epothilone D, possibly leading to product repression and enhanced product degradation rates.

The *M. xanthus* spent resin contains bound methyl oleate at the end of a cultivation but has a significantly higher binding capacity for epothilone D than the *S. cellulosum* resin, which contains no bound oils. GC/MS analysis of the *M. xanthus* resin extract confirmed that a peak elutes which has a retention time (18.3 min) consistent with a methyl oleate standard and a mass consistent with methyl oleate ($m/z = 297$). Although the amount of oil bound by the resin is low relative to the amount of epothilone (4.1 mg/g), it is possible that these hydrophobic oil chains may provide additional binding sites on the resin bead surface for epothilone D,

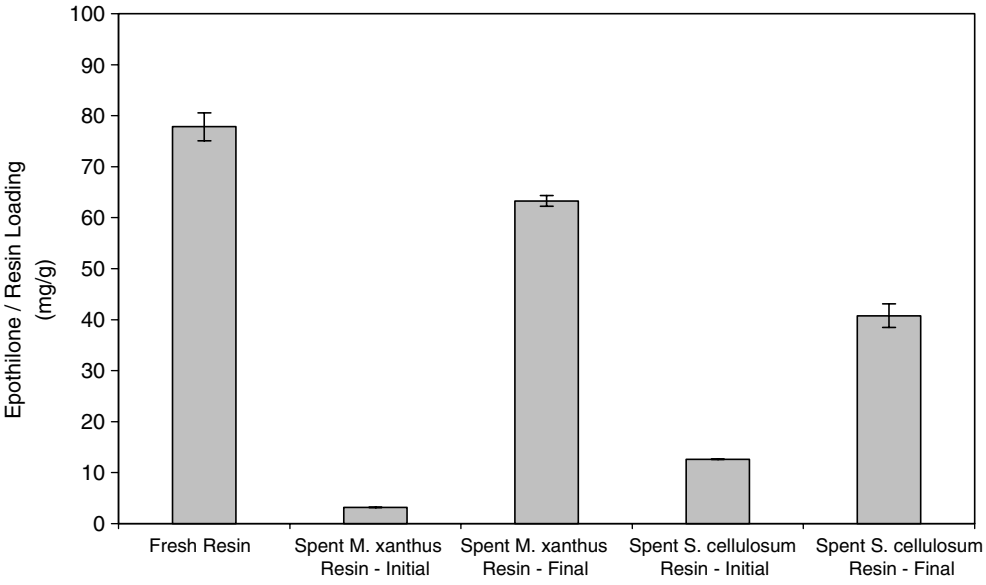

Fig. 2 Loading of epothilones on fresh and spent resins. The *initial data point* for each resin type indicates the amount of product bound to the spent resin following cultivation. The *final data point* indicates the total amount of product associated with the spent resin after its complete saturation with epothilone D. The total binding capacity of the resins for additional epothilone is highly dependent upon the nature of the production strain and process. *Error bars* indicate the standard deviation of each triplicate data set

alleviating the effect of other fouling compounds present on the resin. Spent resin from an *S. cellulosum* cultivation which had been incubated for 1 week with methyl oleate at a concentration of 13.1 mg/g exhibited a 20% higher total epothilone loading capacity than spent resin from the same run which had not been pretreated with methyl oleate (data not shown).

Fracture of product adsorption resin during a microbial cultivation

Typical fed-batch epothilone D production runs occur over a 2-week period [14]. During this long cultivation period, these resin beads are continuously subjected to impact forces caused by collisions with other beads or with internal bioreactor structures, such as the agitation impellers. If these impact forces are sufficiently high, they can cause the fracturing of the resin beads into smaller pieces. The rate and amount of adsorber resin bead fracture occurring will vary with the type of bioreactor as the agitation impeller size, its rate of rotation, and the internal structural setup of a particular bioreactor all contribute to a unique rate of resin fracture.

This experimental problem is similar to studies performed by Cherry and Papoutsakis [3–5] where they investigated the amount of damage done to microcarrier-borne mammalian cells by the shear, bead-bead collision, and impeller impact forces present in a bioreactor. The impeller rotation rate largely determines the acceleration and shear forces present in the microenvironment of a resin bead. Energy is transferred from the impeller blades into various eddy sizes in a turbulent fluid, with the smallest eddy size dissipating its kinetic energy into the fluid through viscous effects [13]. The adsorber resin beads are accelerated by turbulent eddies of approximately the same size as the beads and have a maximal velocity (v) of:

$$v = (d\varepsilon)^{1/3}. \tag{2}$$

Here, d represents the diameter of the resin beads (0.06 cm) and ε is the rate of turbulent energy dissipation per volume of fluid, which is dependent on the impeller rotation rate (n) at steady state [4]:

$$\varepsilon = \frac{N_p n^3 d_i^5}{V}. \tag{3}$$

Here, V represents the liquid volume in the bioreactor, d_i the impeller diameter (6.5 cm), and N_p is the impeller power number, which is a function of the bioreactor configuration and the impeller Reynolds number. An N_p value of 4.22 is assumed from literature, given a similar bioreactor geometric profile and impeller configuration run at a high Reynolds number [12].

The bead-bead collision forces and the volume fraction of the beads in the bioreactor determine the collision rate of resin beads with one another and the force of these collisions. The collision kinetic energy of the beads impacting one another can be calculated by [4]:

$$\text{Bead collision energy} = \frac{1}{2}\left[\rho_b \frac{4}{3}\pi\left(\frac{d}{2}\right)^3\right]\left[(\varepsilon d)^{1/3}\right]^2. \tag{4}$$

The collision energy of these beads at a relatively high agitation rate (800 rpm) is 7×10^{-3} g cm^2/s^2, or approximately five orders of magnitude higher than the threshold shear work resulting in the loss of viability of mammalian cells, estimated to be about 4×10^{-8} g cm^2/s^2 [4]. The resin beads are accelerated to the velocity of eddies of a similar size (0.06 cm), or to approximately 10.9 cm/s at this agitation rate.

The response of a resin bead to an impact force is dependent upon a number of factors, including the strength and ductility of the bead [18]. Mechanical compression studies have been utilized to estimate these

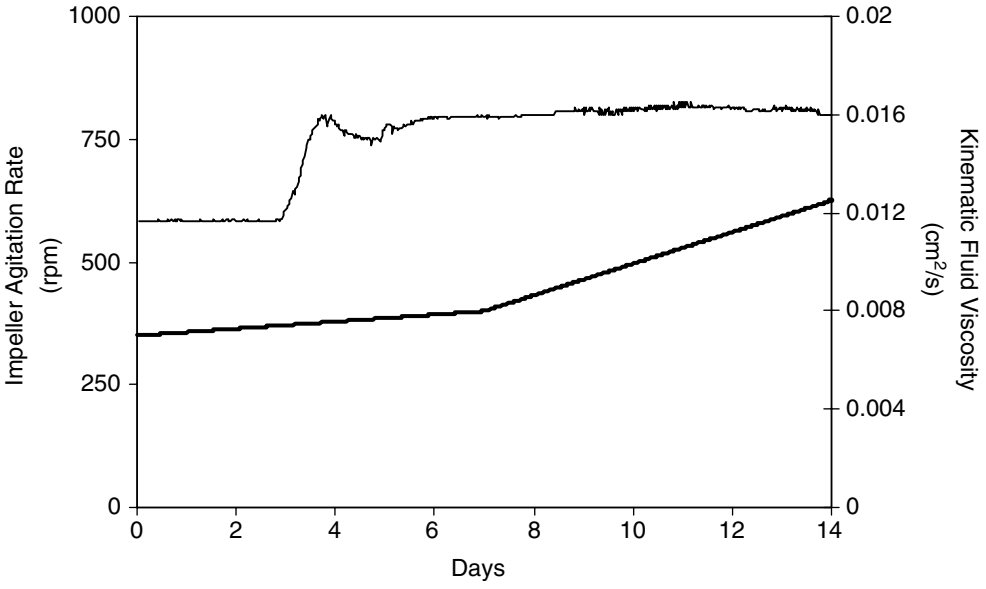

Fig. 3 Agitation rate (*thin line*) and viscosity (*solid line*) profiles of an *S. cellulosum* cultivation and the resin fracture simulation run

values for a single resin bead [2]. The XAD-16 resin was found to be the least ductile and most prone to fracture of the various resin types tested. A compression force of 1 N was required to fracture a representative XAD-16 resin bead under loading, while some of the other resin beads were able to withstand compression forces seven times higher. The polystyrene XAD-16 resin beads deform under a compression load by almost 25% of the bead diameter before fracture occurs [2], or by about 150 μm for an average bead. The threshold amount of work required over this deformation distance for a resin bead to fracture from a single impact is approximately 1.5×10^4 g cm^2/s^2, about six orders of magnitude higher than the actual bead-bead collision energy at an agitation rate of 800 rpm. However, the impact energy of a bead-bead collision is expended in a much shorter time period than in the compression loading studies, likely resulting in a lower required impact force to result in a bead fracture event.

The destructive collision effects on a resin bead in a bioreactor are dependent not only on the force of a bead-bead impact, but also on its frequency. Impacts of sub-fracture collision energies can still result in the accumulation of structural defects within the bead, with the distribution of these internal cracks dependent on the energy of the collision [18]. This results in the weakening of the structural integrity of the bead to the point where lower impact forces become sufficient to result in a fracturing event.

Cherry and Papoutsakis [4] have developed a power correlation called the turbulent collision severity (TCS) to comprehensively describe the kinetic energy of these bead-bead collisions and the specific bead collision frequency per unit of bioreactor volume. The value of α (0.04) represents the volume fraction of the resin beads in the bioreactor.

$$\mathrm{TCS} = \left(\frac{mv^2}{2}\right)\left(\frac{v\alpha^2}{d^4}\right)\left(\frac{(4\pi/3)(d/2)^3}{\alpha}\right). \quad (5)$$

The agitation impeller tip speed (v_{tip}) is almost 25 times higher than the maximum resin bead velocity at an impeller rotation rate of 800 rpm, resulting in much higher collision energies when a resin bead impacts the agitation impeller during a run. A second correlation (the impeller collision severity, or ICS) was also

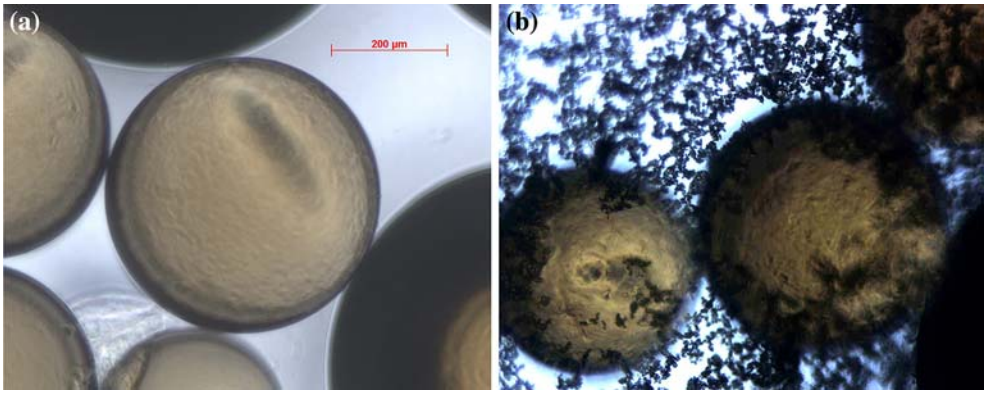

Fig. 4 Microscopic image of XAD-16 resin from the resin fracture simulation run before (**a**) and after (**b**) 7 days of agitation. Image was taken at a total magnification of 100 times

developed [4] to describe the power involved in these collisions:

$$\mathrm{ICS} = \left(\frac{m v_{\mathrm{tip}}^2}{2}\right)\left(\frac{(n_b d_i d/2) v_{\mathrm{tip}}}{V}\right). \quad (6)$$

The ratio between the ICS and TCS values at 800 rpm was approximately 31, indicating that the damage from bead-bead collisions is negligible in comparison to that resulting from bead-impeller collisions. Almost all of the damage done to the resin beads during these myxobacterial cultivations is likely a result of impeller impacts.

Small fragments of the resin beads could be observed microscopically in the culture broth of an epothilone D production cultivation, but were approximately the same size as some of the cellular aggregates present in the sample. These cellular aggregates cannot be accurately discriminated from the resin fragments using laser diffraction resin sizing analysis, so an alternative strategy was used to determine the evolution of the resin bead distribution during an actual cultivation. The cultivation conditions of an epothilone D fed-batch cultivation were simulated in a 5 l bioreactor without the presence of the cell culture to assess the degree of resin fracture occurring during these cultivations. Continuous fragmentation of these beads over a long period of time results in the accumulation of bead fragments in the bioreactor, and a reduction in the median resin bead size over time. This mode of fragmentation has also been observed with pellets of filamentous fungi during cultivation [12, 16, 19, 20].

This resin fracture simulation run was conducted to replicate the impeller agitation rate and viscosity profiles of a typical fed-batch epothilone D production cultivation. The culture viscosity profiles of two identical fed-batch *S. cellulosum* cultivations were determined using an Oswald viscometer and found to increase approximately 50% (from 0.007 to 0.013 cm^2/s) over the 14 days cultivation (Fig. 3). This is due to the increase of the cell concentration during the run and the secretion of extracellular proteins and viscous exopolysaccharides by this myxobacterium [24]. A programmed agitation rate profile for the 5 l bioreactor was used to replicate that of an actual cultivation (Fig. 3), which utilizes an agitation cascade control loop to maintain the dissolved oxygen tension at an appropriate level throughout the run. Additionally, a 70% glycerol solution was pumped in at an appropriate rate to replicate the fed-batch culture viscosity profile (Fig. 3). Small fragments of resin broken off of the beads were readily visible by day 7 (Fig. 4b). The resin particle size distributions of the samples could be determined, as there were no cellular aggregates present to interfere with the analysis.

The relevant resin bead size distribution parameters of the various samples from this run are summarized in Table 1. The median particle diameter represents the bead size in which 50% of the resin beads in the sample are larger or smaller than that particular diameter. Span indicates the polydispersity, or width, of a resin size distribution. Fracturing of the resin beads into smaller particles will result in a reduction in the mean diameter of the resin beads, an increase in the span of the bead distribution, and the accumulation of small (<250 μm diameter) fragments not initially present in the resin bead distribution.

Table 1 Resin particle distribution properties during the simulation cultivation

Days	Agitation rate (rpm)	Median particle diameter (μm)	Span	Percentage of particles <250 μm
0	600	650	0.85	0%
3	615	653	0.89	0%
7	809	630	0.98	4.1%
10	829	586	1.58	18.8%
14	814	551	1.65	28.8%

Temporal evolution profiles of the resin size distributions from this run are shown in Fig. 5. Significant amounts of resin fracture were observed to begin on day 7, and continue throughout the duration of the run. No evidence of significant resin fracture was observed in this run until after the agitation rate was increased from 600 to approximately 800 rpm following day 3 (Fig. 4, Table 1). It is likely that an impeller-bead threshold collision energy exists between these two agitation rates required for resin fragmentation to occur and must be exceeded for fracturing of the resin to initiate.

The size of the resin fragments released from the beads during the run also increased as the run progressed (Fig. 5). This may again be due to fatigue or weakening of the internal resin bead structural integrity from continuous exposure to these collision forces, resulting in larger fragments being released from the beads as the run progresses [17]. As one would expect, the normalized median bead diameter was observed to decrease throughout the simulation run, while the fraction of resin fragments observed in sequential samples increased throughout the run. An interesting correlation arises when these bead population parameters are plotted against a time-integrated ICS profile of the bioreactor run (Eq. 6). This integrated ICS profile represents the aggregate impeller collision energy expended on the resin beads during the entire cultivation (Fig. 6). This correlation may also be used to estimate the resin bead damage occurring in larger 1,000 l epothilone D production bioreactors run under similar cultivation conditions [1]. The final integrated ICS value for a 14 days epothilone D production cultivation at this scale is about 1.2×10^4 g cm^2/s^2, or approximately 70 times lower than the final value in the 5 l simulation run. This would indicate that minimal damage is being done to the XAD resin in the 1,000 l bioreactor cultivation. Indeed, the absence of visible resin fines in the culture broth and quantitative product recovery at harvest indicate that this is the case.

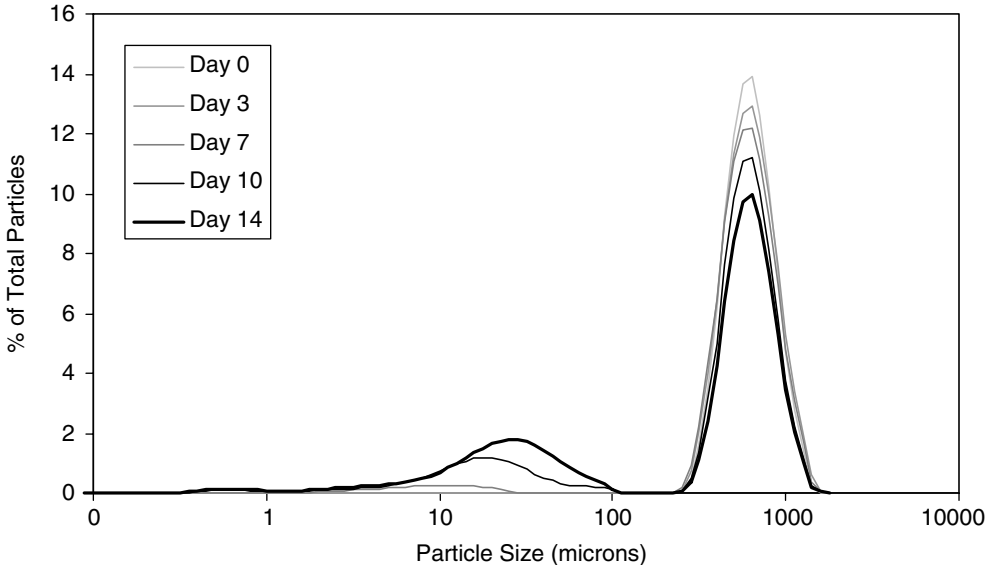

Fig. 5 Resin size distribution temporal evolution during the resin fracture simulation run

Conclusions

XAD-16 adsorber resin was found to be more effective than cyclodextrins for the in situ stabilization of labile small molecules produced during myxobacterial cultivations, resulting in product titers more than twofold higher than those obtained with the cyclodextrins. The resin fouls with various other compounds present in the cultivation medium, but resin samples from the end of two different myxobacterial cultivations still had adequate binding capacity to capture more than three times the product bound by the resin during a typical cultivation.

However, long cultivation times at high impeller agitation rates resulted in significant amounts of resin fracture and the associated product loss occurring during the bioreactor harvest. Microbial cultivations utilizing an in situ adsorber resin product stabilization strategy and the associated bead harvesting process should be designed in such a way to minimize bead fragmentation during cultivation and maximize the amount of resin harvested at the end of a run. The size of the capture mesh used to sieve the resin particles at the end of cultivation should be optimized to capture the maximal number of resin fragments, while not interfering with the passage of the cultivation broth and smaller cellular aggregates through the mesh. Another possibility would be to utilize an alternative resin type possessing a similar product capture capacity as XAD-16, but with a higher mechanical strength and ductility. The cultivation parameters could also be modified to minimize the impeller agitation rate and the duration of the

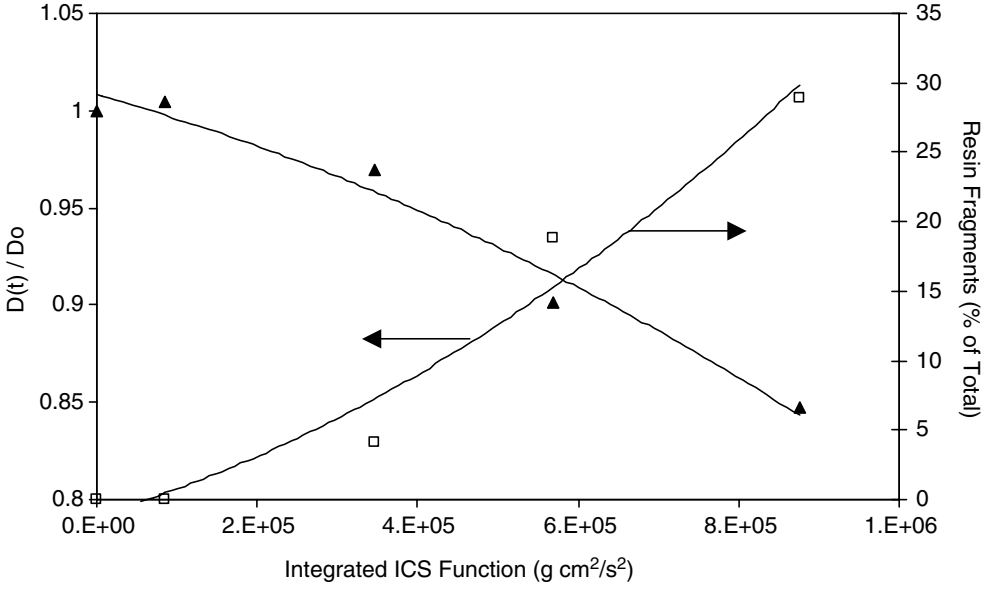

Fig. 6 Correlation of the normalized median diameter ($D(t)/D_o$) of the resin beads (*filled triangle*), and the fraction of resin fragments present in the distribution (*unfilled square*) with the time-integrated ICS. Resin fragments less than 250 μm in diameter are assumed to have fractured from a larger bead during the resin fracture simulation run, as they are not initially present in the bead distribution

cultivation to reduce the impact severity and accumulation of the bead/impeller collisions during the run.

Acknowledgments The authors thank Geoffrey Nosarati for his assistance with the GC/MS analysis of the resin extract samples.

References

1. Arslanian R, Parker C, Wang P, McIntire J, Lau J, Starks C, Licari P (2002) Large-scale isolation and crystallization of epothilone D from *Myxococcus xanthus* cultures. J Nat Prod 65:570–572
2. Breitbach M, Bathen D, Schmidt-Traub H, Ebener H (2002) Stability of adsorber resins under mechanical compression and ultrasonication. Polym Adv Technol 13:391–400
3. Cherry RS, Papoutsakis ET (1986) Hydrodynamic effects on cells in agitated tissue culture reactors. Bioprocess Eng 1:29–41
4. Cherry RS, Papoutsakis ET (1988) Physical mechanisms of cell damage in microcarrier cell culture bioreactors. Biotechnol Bioeng 32:1001–1014
5. Cherry RS, Papoutsakis ET (1989) Growth and death rates of bovine embryonic kidney cells in turbulent microcarrier bioreactors. Bioprocess Eng 4:81–89
6. Chou TC, Zhang XG, Balog A, Su DS, Meng D, Savin K, Bertino JR, Danishefsky SJ (1998) Desoxyepothilone B: an efficacious microtubule-targeted antitumor agent with a promising *in vivo* profile relative to epothilone B. Proc Natl Acad Sci USA 95:9642-9647
7. Gerth K, Washausen P, Höfle G, Irschik H, Reichenbach H (1996a) The jerangolids: a family of new antifungal compounds from *Sorangium cellulosum* (myxobacteria). Production, physico-chemical and biological properties of jerangolid A. J Antibiot 49:71–75
8. Gerth K, Bedorf N, Höfle G, Irschik H, Reichenbach H (1996b) Epothilons A and B: antifungal and cytotoxic compounds from *Sorangium cellulosum* (myxobacteria)—production, physico-chemical, and biological properties. J Antibiot 49:560-563
9. Gerth K, Steinmetz H, Höfle G, Reichenbach H (2002) Studies on the biosynthesis of epothilones: hydroxylation of epo A and B to epothilones E and F. J Antibiot 55:41–45
10. Jumaa M, Carlson B, Chimilio L, Silchenko S, Stella V (2004) Kinetics and mechanism of degradation of Epothilone-D: an experimental anticancer agent. J Pharm Sci 93:2953–2961
11. Julien B, Shah S (2002) Heterologous expression of the epothilone biosynthetic genes in *Myxococcus xanthus*. Antimicrob Agents Chemother 46:2772–2778
12. Jüsten P, Paul GC, Niewnow AW, Thomas CR (1996) Dependence of mycelial morphology on impeller type and agitation intensity. Biotechnol Bioeng 52:672–684
13. Kolmogorov DN (1941) C.R. (Doklady) Acad Sci USSR 30:301–305
14. Lau J, Frykman S, Regentin R, Ou S, Tsuruta H, Licari P (2002) Optimizing the heterologous production of epothilone D in *Myxococcus xanthus*. Biotechnol Bioeng 78:280-288
15. Marshall VP, McWethy SJ, Sirotti JM, Cialdella JI (1990) The effect of neutral resins on the fermentation production of rubradirin. J Ind Microbiol 5:283–288
16. Nielsen J, Johansen CL, Jacobsen M, Krabben P, Villadsen J (1995) Pellet formation and fragmentation in submerged cultures of *Penicillium chrysogenum* and its relation to penicillin production. Biotechnol Prog 11:93–98
17. Pitchumani R, Meesters GMH, Scarlett B (2003) Breakage behavior of enzyme granules in a repeated impact test. Powder Technol 130:421–427
18. Salman AD, Reynolds GK, Mounslow MJ (2003) Particle impact breakage in particulate processing. KONA Powder Particle 21:88–98
19. Smith JJ, Lilly MD, Fox RI (1990) The effect of agitation on the morphology and penicillin production of *Penicillium chrysogenum*. Biotechnol Bioeng 35:1011–1023
20. van Suijdam JC, Metz B (1981) Influence of engineering variables upon the morphology of filamentous molds. Biotechnol Bioeng 23:111–148
21. Warr GA, Veitch JA, Walsh AW, Hesler GA, Pirnik DM, Leet JE, Lin PM, Medina IA, McBrien KD, Forenza S, Clark JM, Lam KS (1996) BMS-182123, a fungal metabolite that inhibits the production of TNF-α by macrophages and monocytes. J Antibiot 49:234–240
22. Woo EJ, Starks CM, Carney JR, Arslanian R, Cadapan L, Zavala S, Licari P (2002) Migrastatin and a new compound, isomigrastatin, from *Streptomyces platensis*. J Antibiot 55:141–146
23. Yang SA, Pyle DL (1999) The adsorption kinetics of cephalosporin-C on non-ionic polymeric macropore Amberlite XAD-16 resin. J Chem Technol Biotechnol 74:216–220
24. Zhang J, Wang R, Jiang P, Liu Z (2002) Production of an exopolysaccharide bioflocculant by *Sorangium cellulosum*. Lett Appl Microbiol 34:178–181